Comparison of the degradation behavior of PLGA scaffolds in micro-channel, shaking, and static conditions

C. H. Ma, H. B. Zhang, S. M. Yang, R. X. Yin, X. J. Yao, and W. J. Zhang

Citation: Biomicrofluidics **12**, 034106 (2018); doi: 10.1063/1.5021394
View online: https://doi.org/10.1063/1.5021394
View Table of Contents: http://aip.scitation.org/toc/bmf/12/3
Published by the American Institute of Physics

Comparison of the degradation behavior of PLGA scaffolds in micro-channel, shaking, and static conditions

C. H. Ma,[1] H. B. Zhang,[1,a)] S. M. Yang,[2] R. X. Yin,[1] X. J. Yao,[1] and W. J. Zhang[3]

[1]*School of Mechanical and Power Engineering, East China University of Science and Technology, Shanghai 200237, China*
[2]*School of Mechatronics and Automation, Shanghai University, Shanghai, China*
[3]*Division of Biomedical Engineering, University of Saskatchewan, Saskatoon S7N 5A9, Canada*

(Received 4 January 2018; accepted 1 May 2018; published online 18 May 2018)

Degradation of scaffolds is an important problem in tissue regeneration management. This paper reports a comparative study on degradation of the printed 3D poly (lactic-co-glycolic acid) scaffold under three conditions, namely, micro-channel, incubator static, and incubator shaking in the phosphate buffer saline (PBS) solution. In the case of the micro-channel condition, the solution was circulated. The following attributes of the scaffold and the solution were measured, including the mass or weight loss, water uptake, morphological and structural changes, and porosity change of the scaffold and the pH value of the PBS solution. In addition, shear stress in the scaffold under the micro-channel condition at the initial time was calculated with Computational Fluid Dynamics (CFD) to see how the shear stress factor may affect the morphological change of the scaffold. The results showed that the aforementioned attributes in the condition of the micro-channel were significantly different from the other two conditions. The mechanisms that account for the results were proposed. The reasons behind the results were explored. The main contributions of the study were (1) new observations of the degradation behavior of the scaffold under the micro-channel condition compared with the conditions of incubator static and incubator shaking along with underlying reasons, (2) new understanding of the role of the shear stress in the scaffold under the condition of the micro-channel to the morphological change of the scaffold, and (3) new understanding of interactions among the attributes pertinent to scaffold degradation, such as weight loss, water uptake, pH value, porosity change, and morphological change. This study sheds important light on the scaffold degradation to be controlled more precisely. *Published by AIP Publishing.* https://doi.org/10.1063/1.5021394

I. INTRODUCTION

The three-dimensional porous scaffolds of biodegradable aliphatic polyesters such as poly (lactic-co-glycolic acid) (PLGA) have been widely used as temporary extracellular matrices in tissue engineering.[1,2] The degradation behavior of the PLGA scaffolds is very important in tissue regeneration; for example, the degradation rate of the porous scaffolds may affect cell growth, cell vitality, and even host response.[3] A porous scaffold should maintain its mechanical properties and structural integrity in agreement with cell growth; a scaffold is desired to be completely degraded by the body after the scaffold accomplishes its mission.[4,5]

The degradation rate of PLGA scaffolds can be measured by weight loss or mass loss, porosity change, surface wrinkling, body distortion, and pore size change,[6,7] and these measures are further related to the structure of PLGA scaffolds such as the shape and level of

[a)]Author to whom correspondence should be addressed: hbzhang@ecust.edu.cn

crystallinity and the composition of poly(glycolic acid) (PGA) and poly(lactic acid) (PLA) (particularly, the higher the hydrophilic PGA content the faster the degradation rate of PLGA.[8–12]). Furthermore, the chemical and biochemical environment also has impacts on the scaffold degradation. For example, the pH value and temperature of a medium along with its enzymatic activity were found to have significant impacts on degradation.[13–15]

Mechanical loads are found to be influential over the degradation of scaffolds.[16–20] Guo *et al.*[21] developed a model to describe the relationship between the tensile stress and degradation rate of the PLGA membrane during the degradation. Dynamic fluid conditions, which generate dynamic mechanical loads on PLGA scaffolds, may have a different effect on the degradation of PLGA scaffolds other than static load.[22,23] Agrawal *et al.*[22] studied the degradation of PLGA scaffolds which have different porosities in a dynamic bioreactor environment. Their results have shown that (1) the degradation under the dynamic fluid condition was slower than that under the static load condition, (2) the molecular weight decreased fast at the beginning and then kept constant after 4 weeks, and (3) there was no much difference between the dynamic load and static load conditions in terms of molecular weight. In Heljak *et al.*'s work,[23] both weight loss and molecular weight change were numerically analyzed in a dynamic bioreactor environment, where the flow rate and the frequency of medium change were analyzed. They found that the effect of the flow rate had a negligible effect on the degradation rate in terms of molecular weight, and furthermore, the porosity was unchanged during the degradation process.

In recent years, a microfluidic 3D perfusion system, in which a scaffold is placed, has been explored[24,25] because of its promise to create a stable, well-defined, and more biologically relevant culture environment for cellular assays and for its excellent research vehicle used for evaluating the effects of various environmental factors on cell physiology.[26–33] Additionally, the microfluidic cell culture system has the benefits of (1) the small physical size of the environment, (2) the possibility to manipulate fluids with a precise spatiotemporal resolution, (3) the provision of a simulated *in vivo* cellular microenvironment, and (4) the low consumption of resources for research due to its need of small volumes of cells and drugs.

The microfluidic bioreactor or condition (or micro-channel for simplicity) may have nontrivial differences from the bioreactor or the incubator which is subject to mechanical shaking (or called incubator shaking for simplicity) although both have significant movements of fluids on the scaffold which sits in the micro-channel or incubator shaking environment. Yet, in the latter case, the fluid flow is not circulated. The foregoing difference in the fluid movement between the micro-channel and the incubator shaking environment has not been paid attention in the literature. To our best knowledge, there is nobody in the literature who compared scaffold degradation in three conditions: (1) micro-channel, (2) incubator static or stable, and (3) incubator shaking. Missing of this knowledge limits our understanding of the benefit of the micro-channel environment which embraces a scaffold for cell culture and drug delivery, along with the underlying reason. Furthermore, there is nobody in the literature who examined how the shear stress in the scaffold may affect the degradation of the scaffold in the micro-channel environment or condition.

In this paper, a comparative study of the degradation of PLGA scaffolds under the three conditions is presented. The following attributes of the scaffold and the solution were measured, such as the mass or weight loss, water uptake, morphological and structural changes, and porosity change of the scaffold and the pH value of the phosphate buffer saline (PBS) solution. Additionally, the shear stress in the scaffold under the micro-channel condition at the initial time was calculated with Computational Fluid Dynamics (CFD) to see how the shear stress may affect the morphological change of the scaffold.

II. MATERIALS AND METHODS

A. Materials

The PLGA powder (copolymerization ratio of PLA/PGA = 50/50) was purchased from Jinan Daigang Biomaterial Co. Ltd., China. The average molecular weight was about 7×10^4 Da, and the polydispersity index was about 1.5. The 3D bioplotter (Envision Tec.

Germany) was used to fabricate the 3D porous PLGA scaffolds. The culture medium was PBS solution (pH value: 7.4 at 37 °C). The viscosity of PBS solution was 1.45×10^{-3} Pa s.[34]

B. Preparation of the 3D porous PLGA scaffold

The cartridge of the 3D printer was filled with PLGA and heated to 180 °C prior to printing. Scaffolds of 6 mm in diameter and 550 μm in spacing were constructed. The first layer was laid on a slide using the syringe dispenser with the nozzle inner diameter of 200 μm. Each subsequent layer was printed to the surface of the partially solidified previous layer after the lifting of the dispenser along the Z axis. This was repeated 5 times to obtain a 6-layer porous structure. The linear speed of the dispenser movement along the X and Y axes was set to be 3 mm/s, and the pressure was set to be 2 bar. The thickness of an individual matrix layer was approximately 250 μm, and the standard deviation was 10.76 μm.

C. Preparation of the test environments

1. Micro-channel environment

The setup of the micro-channel environment is shown in Fig. 1. It is composed of the following parts: a peristaltic pump (Masterflex L/S; Cole-Parmer), a custom-made microfluidic device, and a gas remover used to remove bubbles in the culture medium. PBS was circulated by a peristaltic pump. The microfluidic device consisted of a micro-channel made of multilayers of polydimethylsiloxane (PDMS) and two polymethylmethacrylate (PMMA) sheets, as shown in Fig. 1(b). The dimensions of the flow chamber are as follows: D = W = 2 mm, L = 60 mm, R = 4.5 mm, and d = 6 mm [Fig. 1(c)].

The microfluidic device was placed in an incubator to maintain a constant temperature of 37 °C. Figure 1(c) shows the microfluidic device used in this study. The flow rate of the micro-channel inlet was 0.029 ml/min and the flow velocity was approximately 1.2×10^{-4} m/s, which are commonly used in bioreactors.[20]

The numerical simulation of the fluid flow in the microfluidic perfusion system (or micro-channel) was carried out using a finite volume technique along with a commercial package (FLUENT6.3.26; ANSYS, Canonsburg, PA).

2. Incubator static and incubator shaking environment

The incubator static condition was constructed as follows: A bottle was taken as an incubator that contains 20 ml PBS solutions, and a scaffold was placed in the bottle. To establish the incubator shaking condition, the bottle was mounted on a platform (the X-Y plane) that was rotated around the Z axis at the rate of 100 rpm/min. The velocity near the wall of the bottle (or incubator) was 1.67 m/s.

D. In vitro degradation measurement

In its very nature, the degradation refers to weight loss.[5] The *in vitro* degradation measurement of the scaffold was performed for up to 4 weeks in the micro-channel, incubator static, and incubator shaking environments or conditions. The instrument to measure the weight was an electrical balancer (BSA224S-CW, Sartorius). The scaffold was taken out from the PBS solution. The wet weight (m_w) of the scaffold was measured after wiping off the surface water on the scaffold. The scaffold was then washed with distilled water and dried in vacuum for 48 h, and the static pressure of the vacuum oven was 50 Pa. The dried mass (m_d) was then measured using the electrical balancer.

E. Characterization studies

1. pH values

The pH values of the PBS solutions along with the scaffolds in the micro-channel, incubator static, and incubator shaking environments were obtained every seven days using the SX-

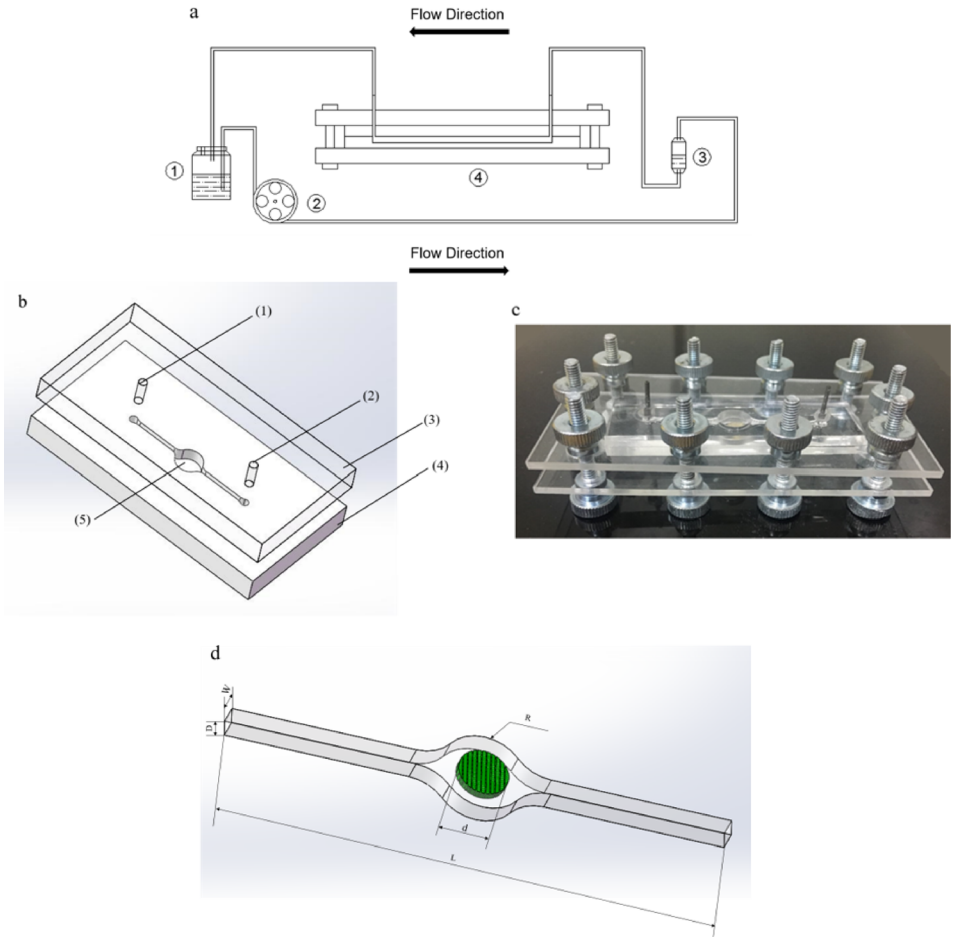

FIG. 1. The microfluidic 3D perfusion system. (a) Schematic diagram of the microfluidic 3D perfusion system: ① Culture media reservoir, ② peristaltic pump, ③ gas remover, and ④ microfluidic device. (b) Microfluidic device: (1) inlet joint, (2) outlet joint, (3) top PDMS layer, (4) bottom PDMS layer, and (5) culture chamber. (c) Prototype of the microfluidic device. (d) Dimensions of the culture chamber (D = W = 2 mm, L = 60 mm, R = 4.5 mm, and d = 6 mm).

620 pH Tester. The specific procedure of the measurement was as follows: first, the pH tester was calibrated before each test, and next, the electrode was immersed into the test solution until the pH value was stable enough to obtain the pH values.

2. Water uptake, mass loss, and porosity change

The scaffolds were taken out from the PBS solution in time intervals and weighed to obtain the wet weight (m_w) and dry weight (m_d). The water uptake of the scaffold was calculated by

$$\%\,\text{water uptake} = \left(\frac{m_w - m_d}{m_d}\right) \times 100\%. \tag{1}$$

The initial mass of the scaffold (m_o) was measured before it was immersed in the culture medium (PBS solutions), and the mass loss of the scaffold after degradation for a certain period of time was then calculated by

$$\%\text{mass loss} = \left(\frac{m_o - m_d}{m_o}\right) \times 100\%. \tag{2}$$

The porosity of the scaffold was measured using the software ImageJ.

3. Morphology

The macromorphology of the scaffold in the micro-channel, incubator static, and incubator shaking conditions during the degradation of the scaffold was observed. The scanning electron microscopy (SEM) images were taken using a Philips XL30 SEM after gold coating.

III. RESULTS

A. Numerical simulation of fluid flow

Figure 2 shows the results of the numerical simulation of the fluid flow within the micro-channel. From Fig. 2(a), it can be seen that the flow streamlines went through the scaffold, implying that there was a strong perfusion inside the scaffold. A strong perfusion would likely produce a relatively high shear stress on the surfaces of the strands near the edge of the scaffold, as shown in Fig. 2(b). The shear stress near the outer edge of the scaffold was larger than that in the center region, and the highest shear stress reached to 1 mPa at the edge of the scaffold, while the lowest shear stress inside the porous material was only 10^{-6} mPa.

B. pH value

Figure 3 exhibits the variation of the pH value of PBS solution during the degradation of scaffolds in the three conditions: incubator shaking, incubator static, and micro-channel. It can be seen from Fig. 3 that the pH values of the PBS solution decreased gradually during degradation in all the three cases. However, a decrease in the pH value in the micro-channel condition was the slowest, from 7.4 to 6.8, followed by the incubator shaking condition, from 7.4 to 3.7, and by the incubator static condition, from 7.4 to 3.1.

C. Water uptake

Figure 3(b) shows the changes in water uptake during the degradation of the PLGA scaffolds in the three conditions (incubator shaking, incubator static, and micro-channel). The results indicate that in all the three conditions, water uptake experienced a trend from increase to decrease. In the case of the scaffold in the incubator shaking condition, water uptake increased dramatically, especially increasing sharply during the first 14 days to the peak of 485%, from 14 days to 21 days and after that period decreased gradually and then decreased sharply. The increase rate of water uptake with the scaffold in the micro-channel condition was the slowest; it reached the maximum of 234% on day 21, began to decrease gradually, and reached below zero until the last day of degradation. While in the case of the scaffold in the incubator static condition, water uptake increased rapidly during the first three weeks. After 14 days, water uptake began to decrease drastically; on the last day of degradation, water uptake reached below zero.

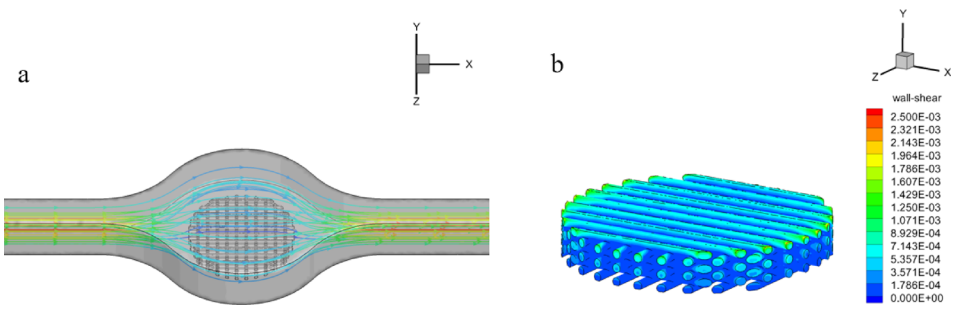

FIG. 2. CFD simulation results in the micro-channel environment: (a) streamline distribution in the micro-channel and (b) the surface shear stress distribution of the scaffold.

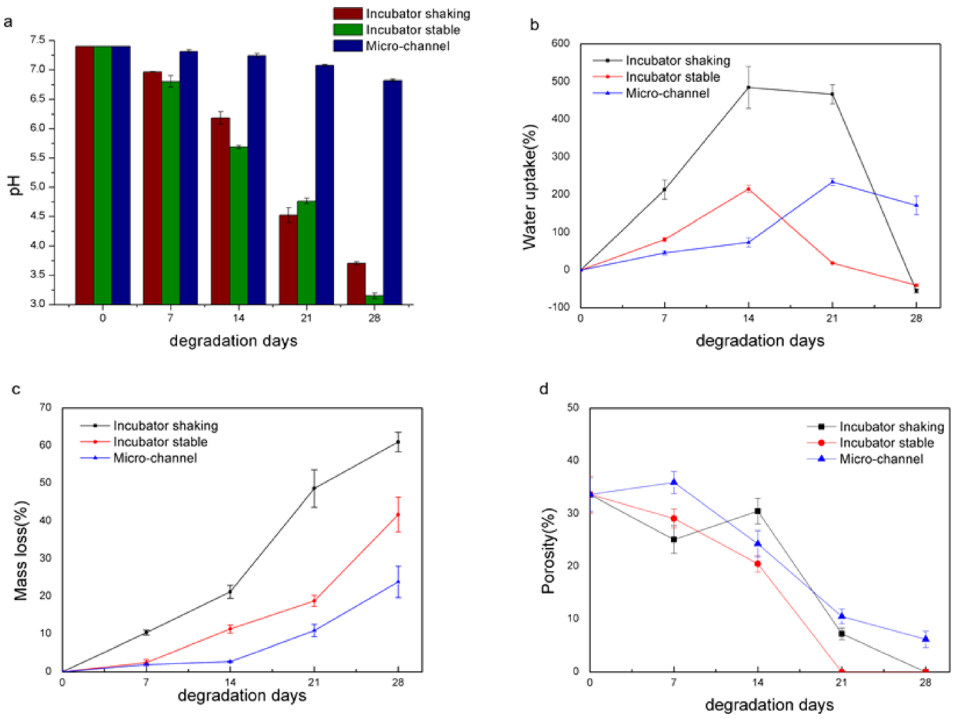

FIG. 3. Degradation characteristics of scaffolds in the micro-channel, incubator static, and incubator shaking conditions: (a) pH value of the PBS solution during degradation, (b) water uptake of the PLGA porous scaffolds during degradation, (c) mass loss of the PLGA porous scaffolds during degradation, and (d) porosity of the PLGA porous scaffolds during degradation.

D. Mass loss

Figure 3(c) shows that the mass losses of all the three conditions tended to decrease during degradation; however, the amount of mass loss in the case of the incubator shaking condition was the highest: particularly, mass loss sharply increased from 14 days, and at the end of the degradation period, the mass loss reached 61.0%. As for the mass loss of the scaffold in the incubator static condition, it increased slightly from the first 7 days, and on day 21, the mass loss increased sharply and reached 41.7% at the end of degradation. In the micro-channel condition, the rate of mass loss was the lowest: particularly for the first 14 days, the rate of mass loss was very low, and from the 14 days, mass loss increased remarkably, and on the day 28, mass loss reached the maximum of 23.8%.

E. Porosity change

Figure 3(d) shows changes in the porosity during the degradation of the scaffold in the three conditions. It can be seen from Fig. 3(d) that (1) the porosity of the scaffold decreased gradually in all the three conditions, (2) the porosity of the scaffold in the micro-channel condition was the highest among the three conditions especially at the later stage of degradation on day 21 and day 28, and (3) the porosity of the scaffold decreased to zero on day 21 and day 28 in the incubator static and incubator shaking conditions, respectively; yet in the micro-channel condition, the porosity maintained at 8% even on the last day.

F. Macromorphology

The morphology in the context of this work includes the surface characteristics and the structure. The macromorphology of the scaffold in the micro-channel, incubator static, and incubator shaking conditions is shown in Fig. 4(A). In the case of the scaffolds in the micro-channel condition, it can be seen from Fig. 4(A) that the maximum water uptake occurred on

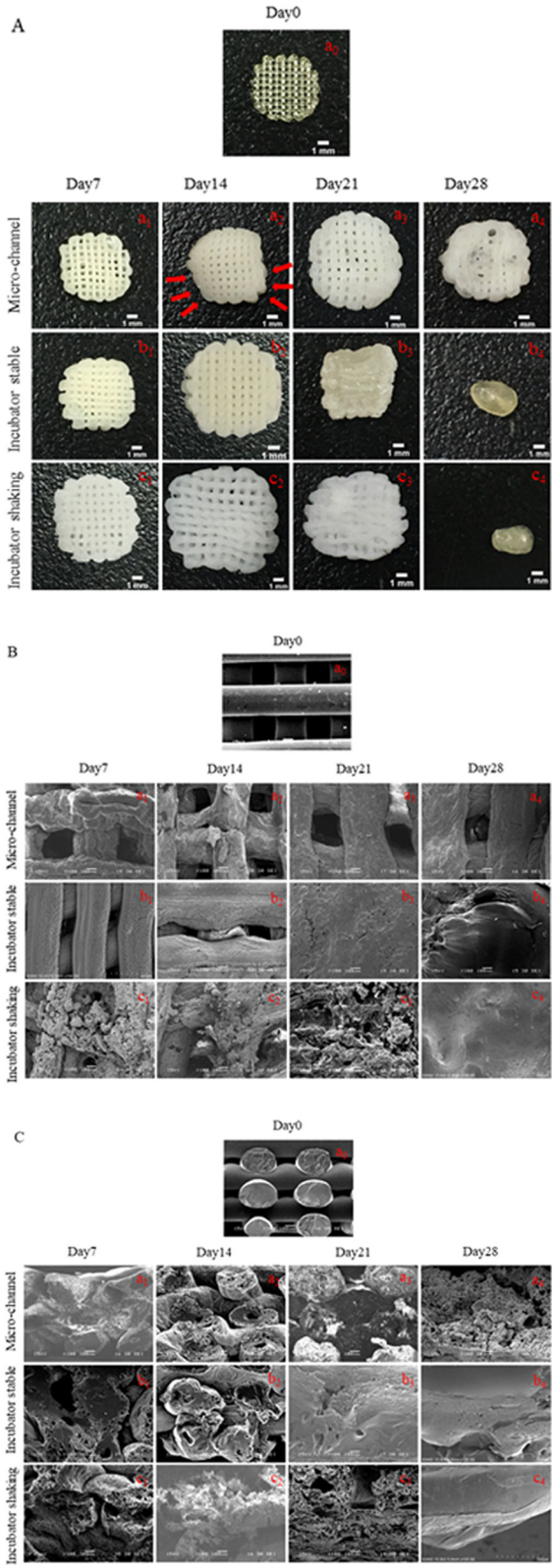

FIG. 4. The macromorphology and scanning electron microscopy morphology of the PLGA porous scaffolds during degradation: (A) the macromorphology of the PLGA porous scaffolds during degradation, (B) the surface SEM morphology of the PLGA porous scaffolds during degradation, and (C) the cross-sectional SEM morphology of the PLGA porous scaffolds during degradation. Red arrows indicate the premature closure of the pores at the edge.

day 21 and that the scaffolds maintained a relatively good pore structure during the entire degradation process; however, the pores at the edge of the scaffolds were closed up, which is in good correlation with the result of the shear stress (i.e., the maximum shear stress on the edge of the scaffold; see Fig. 2 and the discussion in Sec. III A). This correlation suggests that the higher the shear stress in the scaffolds, the faster the degradation of the PLGA scaffold. Furthermore, in the case of scaffolds in the incubator static condition, the maximum water uptake occurred on day 14, and on day 21, the scaffolds began to shrink and the pore structure disappeared. On the last day of degradation, the scaffold shrank into a solid piece. Compared with the other two conditions, the scaffolds in the incubator shaking condition exhibited the highest water uptake, and the maximum water uptake occurred on day 14, similar to the scaffold in the incubator static condition. The pore structure of the scaffold began to disappear on day 21, and on day 28, the scaffold shrank to one solid piece.

G. SEM morphology

The morphology change of the surface and the cross section of the PLGA scaffolds before and after degradation are shown in Figs. 4(B) and 4(C), respectively. From Fig. 4(B), it can be seen that the surface of the scaffold was smooth when it was printed. In the case of the scaffold in the micro-channel condition, the scaffold strands swelled during the degradation process, yet the pore structure (especially in the central region) maintained well until the last day of the degradation process. The uneven change of the pore structure of the PLGA scaffold in this case correlates well with the uneven distribution of the shear stress in the scaffold (see Fig. 2). In the case of the scaffold in the incubator static condition, the water uptake of the scaffold reached a maximum on day 14, and from day 21, the pores of the scaffold disappeared, and the surface tended to be flat. In the case of the scaffold in the incubator shaking condition, the change in the morphology of the scaffold was remarkable: there are some cracks on the strands of the scaffold from day 7, and the cracks deepened dramatically as the degradation was progressing.

From the SEM images of the cross-section [i.e., Fig. 4(C)], it can be seen that in the case of the scaffold in the micro-channel condition, the pillars in the scaffold were bulk eroded by the PBS (i.e., small holes were first visible in the center of the stands in the scaffold), and as the degradation was progressing, the holes were denser. In the case of the scaffold in the incubator static and incubator shaking conditions, the bulk erosion phenomenon was similar to that in the case with the micro-channel condition, but the erosion rates were faster, especially in the case of the incubator shaking condition, there were a large number of holes in the cross-section of the scaffold even just in 7 days. Additionally, on the last day of the degradation, the regular structure of the scaffold disappeared and the scaffold appeared to be flat after 21 days in both the incubator shaking and incubator stable conditions; nevertheless, this occurred earlier in the case of the scaffold in the incubator stable condition than in the case of the scaffold in the incubator shaking condition.

IV. DISCUSSIONS

Based on the results obtained and the existing theory in the literature, we propose the following theory or mechanism that may govern the degradation (weight loss) and the structure change of the PLGA scaffold with PBS solution in the three conditions (micro-channel, incubator static, and incubator shaking).

- Governing Principle: the weight loss of the PLGA scaffold is due to the chemical reason between the PLGA material and PBS solution. In such a chemical reaction, polymer chains are broken down to oligomers and monomers, and the autocatalytic reaction may also present, which accelerates the degradation (the lower the pH value, the faster the degradation).[35,36]
- Dominating factor I (the stress factor): the flow of the solution produces mechanical loads on the PLGA scaffolds, which subsequently creates stresses on the PLGA scaffolds and increases the weight loss due to increased water contact and activation energy.[37]

- Dominating factor II (the flow perfusion factor): the flow of the solution dilutes the solution, so as to maintain the pH value of the solution, to reduce the rate of weight loss and to maintain the porosity. It is noted that after long chains of the PLGA are broken to oligomers and monomers, the acidity of the solution increases, so as to increase the rate of weight loss (due to accelerated autocatalytic reaction) and to reduce the porosity.

The above theories nicely explain the phenomena observed from the results of the experiments (Figs. 3 and 4). First of all, the Governing Principle is at play to all the three conditions particularly on weight loss and then to other structural and morphological attributes.

Second, the dominating factor II is responsible for the result as shown in Fig. 3(a). The pH value of the solution decreased with time because the byproduct from the scaffold during the degradation process is acidic. In the case of the scaffold in the micro-channel, the fluid circulates, and the flow takes away the acidic substances and thus reduces the decreasing rate of the pH value in the PBS solution. However, in both the incubator shaking and incubator static conditions, there is no such a flow effect (i.e., carrying-away the degraded substance), and so, the pH values of the solution in these two conditions are of no significant difference and are lower than the pH value in the micro-channel condition. The change behavior of the pH value has given evidence that the Governing Principle is at play (see the first point in the above discussion).

Third, the weight loss of the scaffold in the incubator shaking condition is higher than that in the incubator static condition over the whole degradation period [Fig. 3(c)]. This is because on one hand, the pH values of these two conditions (i.e., incubator static and incubator shaking) are close [Fig. 3(a)], and thus, the scaffolds in these two conditions share the similar degradation process which is governed by the Governing Principle; on the other hand, the stress in the scaffold in the incubator shaking condition is certainly higher than that in the incubator static condition, and the scaffold in the incubator shaking condition degrades faster than that in the incubator static condition (due to the dominating factor I). It is also noted that the dynamic load on the scaffold in the micro-channel condition is symmetric and uniform, and therefore, the stress in the polymer chain bond may not be a significant factor, which is partially responsible for the fact that the weight loss of the scaffold in the micro-channel condition is the lowest [Fig. 3(c)].

Fourth, the underlying reason for the result of Fig. 3(d) regarding the porosity can be explored by the three proposed theories in an integrated manner. In Fig. 3(d), the porosity in the micro-channel condition is the highest except in the short period time (around day 14) at the beginning. This exception may be due to a conflicting role with dynamic load on the scaffold, i.e.,: on one hand, dynamic load may maintain the porosity because the autocatalytic effect was reduced when fluid flow takes away the acidic byproducts, and on the other hand, dynamic load reduces the porosity especially at the edge of the scaffolds [Fig. 4(A)] because dynamic load produces more stress on the scaffold and accelerates mass loss (relevant to the dominating factor I). It is this conflicting role that creates uncertainty to the porosity such that around day 14, the porosity in the incubator shaking condition is higher than that in the micro-channel condition. It is noted that the result of porosity in Fig. 3(d) is correlative well with the result of the morphology in Fig. 4(A), that is, the porosity of the scaffold under the incubator shaking condition appears to be the highest around day 14 among all the three conditions.

Finally, regarding Fig. 4, first, Fig. 4(A) is correlative with the porosity in Fig. 3(d), that is, the porosity of the scaffold in the micro-channel condition is overall highest among all the three conditions except that around day 14, and on day 14, the porosity in the incubator shaking condition is the highest among the three conditions [see Fig. 4(A), the SEM at day 14]. In fact, there is also some correlation of the porosity of Fig. 3(d) with Fig. 4(B) and Fig. 4(C). Second, from Fig. 4(A), it can be seen that more pores on the edge are closed as opposed to pores inside the scaffold for all the three conditions, and this is more a case in the micro-channel condition. This is supported by the information of the shear stress in the scaffold, i.e., the shear stress on the peripheral of the scaffold is higher than that on the surface of the inside strands of the scaffold (Fig. 2). Finally, the perfusion effect associated with the micro-channel condition is

likely responsible for the difference in the change of the structure and the surface of the scaffold, as shown in Figs. 4(B) and 4(C), i.e., the structural integrity of the scaffold in the micro-channel condition is the best among all three conditions, followed by that in the incubator shaking condition and that in the incubator static condition.

V. CONCLUSION

This paper presents a comparative study of degradation of the 3D printed porous PLGA scaffold in PBS solution for three conditions, namely, (1) incubator static, (2) micro-channel, and (3) incubator shaking. The following attributes of the scaffold and the solution were measured, including the mass or weight loss, water uptake, morphological and structural change, and porosity change of the scaffold and the pH value of the PBS solution. Additionally, the shear stress on the scaffold under the micro-channel condition at the initial time was also calculated with CFD to see how the shear stress may affect the morphological change of the scaffold.

The following conclusions are drawn from this study: There are two dominating factors affecting degradation of the scaffold in a micro-channel along with a circulation flow of the PBS solution, which are the stress factor (dominating factor I) and the flow perfusion factor (dominating factor II), and these two factors play them in a combined manner affecting the degradation process.

The main contribution of this study in the field of scaffold engineering is that this study has provided an much improved understanding of the effects of dynamic loading, especially the dynamic interaction of the fluid flow with the scaffold, on degradation of the scaffold both in a micro-channel environment along with a circulating fluid flow and in an incubator shaking environment which contains the fluid (so, the fluid is shaking as well).

In future, we will further study (1) how the flow movement parameter (e.g., flow rate) may affect the degradation behavior in the micro-channel condition with a circulating flow, (2) the behavior of the fluid flow into the scaffold (the scaffold can be viewed as a regular porous medium,[38,39] (3) the change of the structural property such as stiffness[40] under dynamic loading in a micro-channel with a circulating flow, and (4) the culturing behavior of cells in the micro-channel condition with a circulating flow. It is noted that the ultimate goal of our study is to design the scaffold and its environment to control degradation or drug delivery process.

ACKNOWLEDGMENTS

The authors would like to thank the following for their financial support: the Shanghai Lianmeng Grant (No. LM201603) and the Opening project of Shanghai Key Laboratory of Orthopedic Implant (KFKT2016001). This work was in part sponsored by the Natural Science Foundation of Shanghai (15ZR1409300), China.

[1]B. S. Kim and D. J. Mooney, "Development of biocompatible synthetic extracellular matrices for tissue engineering," Trends Biotechnol. **16**, 224–230 (1998).
[2]C. M. Agrawal and R. B. Ray, "Biodegradable polymer scaffolds for musculoskeletal tissue engineering," J. Biomed. Mater. Res. **55**, 141–150 (2001).
[3]J. E. Babensee, J. M. Anderso, L. V. Melntire, and A. G. Mikos, "Host response to tissue engineered devices," Adv. Drug Delivery Rev. **33**, 111–139 (1998).
[4]J. C. Middleton and A. J. Tipton, "Synthetic biodegradable polymers as orthopedic devices," Biomaterials **21**, 2335–2346 (2000).
[5]H. B. Zhang, L. Zhou, and W. J. Zhang, "Control of scaffold degradation in tissue engineering: A review," Tissue Eng., Part B Rev. **20**(5), 492–502 (2014).
[6]A. Göpferich, "Mechanisms of polymer degradation and erosion," Biomaterials **17**, 103–114 (1996).
[7]F. Von Burkersroda, L. Schedl, and A. Göpferich, "Why degradable polymers undergo surface erosion or bulk erosion," Biomaterials **23**, 4221–4231 (2002).
[8]T. G. Park, "Degradation of poly(lactic-co-glycolic acid) microspheres: Effect of copolymer composition," Biomaterials **16**, 1123–1130 (1995).
[9]T. G. Park, "Degradation of poly(D,L-lactic acid) microspheres: Effect of molecular weight," J. Controlled Release **30**, 161–173 (1994).
[10]K. A. Athanasiou, J. P. Schmitz, and C. M. Agrawal, "The effect of porosity on in vitro degradation of polylactic acid-polyglycolic acid implants used in repair of particular cartilage," Tissue Eng. **4**, 53–63 (1998).

[11]S. Hurrell and R. E. Cameron, "The effect of initial polymer morphology on the degradation and drug release from polyglycolide," Biomaterials **23**, 2401–2409 (2002).
[12]J. C. Victor and X. M. Peter, "The effect of surface area on the degradation rate of nanofibrous poly(l-lactic acid) foams," Biomaterials **27**, 3708–3715 (2006).
[13]C. M. Agrawal, D. Huang, J. P. Schmitz, and K. A. Athanasiou, "Elevated temperature degradation of a 50:50 copolymer of PLA–PGA," Tissue Eng. **3**, 345–352 (1997).
[14]Z. S. Banu and D. J. Burgess, "Effect of acidic pH on PLGA microsphere degradation and release," J. Controlled Release **122**, 338–344 (2007).
[15]S. M. Li, A. Girard, H. Garreau, and M. Vert, "Enzymatic degradation of polylactide stereocopolymers with predominant D-lactyl contents," Polym. Degrad. Stab. **71**, 61–67 (2001).
[16]N. D. Miller and D. F. Williams, "The in vivo and in vitro degradation of poly(glycolic acid) suture material as a function of applied strain," Biomaterials **5**, 365–368 (1984).
[17]R. X. Yin, N. Zhang, K. M. Wang, H. Long, T. L. Xing, J. Nie, H. B. Zhang, and W. J. Zhang, "Material design and photo-regulated hydrolytic degradation behavior of tissue engineering scaffolds fabricated via 3D fiber deposition," J. Mater. Chem. B **5**, 329–340 (2017).
[18]S. P. Zhong, P. J. Doherty, and D. F. Williams, "The effects of applied strain on the degradation of absorbable suture in vitro," Clin. Mater. **14**, 183–189 (1993).
[19]M. Deng, J. Zhou, G. Chen, D. Burkley, Y. Xu, D. Jamiolkowski, and T. Barbolt, "Effect of load and temperature on *in vitro* degradation of poly(glycolide-co-l-lactide) multifilament braids," Biomaterials **26**, 4327–4336 (2005).
[20]M. Deng, G. Chen, D. Burkley, J. Zhou, D. Jamiolkowski, Y. Xu, and R. Vetrecin, "A study on in vitro degradation behavior of a poly(glycolide-co-l-lactide) monofilament," Acta Biomater. **4**, 1382–1391 (2008).
[21]M. Guo, Z. W. Chu, J. Yao, W. T. Feng, Y. X. Wang, L. Z. Wang, and Y. B. Fan, "The effects of tensile stress on degradation of biodegradable PLGA membranes: A quantitative study," Polym. Degrad. Stab. **124**, 95–100 (2016).
[22]C. M. Agrawal, J. S. McKinney, D. Lanctot, and K. A. Athanasiou, "Effects of fluid flow on the in vitro degradation kinetics of biodegradable scaffolds for tissue engineering," Biomaterials **21**, 2443–2452 (2000).
[23]M. K. Heljak, W. Swieszkowski, and K. J. Kurzydlowski, "Modeling of the degradation kinetics of biodegradable scaffolds: The effects of the environmental conditions," J. Appl. Polym. Sci. **131**, 40280 (2014).
[24]M. H. Wu, S. B. Huang, and Z. F. Cui, "Development of perfusion-based micro 3-D cell culture platform and its application for high throughput drug testing," Sens. Actuators, B **129**, 231–240 (2008).
[25]M. H. Wu, S. B. Huang, Z. F. Cui, and Z. Cui, "A high throughput perfusion-based microbioreactor platform integrated with pneumatic micropumps for three-dimensional cell culture," Biomed. Microdevices **10**, 309–319 (2008).
[26]T. J. Maguire, E. Novik, and P. Chao, "Design and application of microfluidic systems for in vitro pharmacokinetic evaluation of drug candidate," Drug. Metab. **10**, 1192–1199 (2009).
[27]S. B. Huang, M. H. Wu, S. S. Wang, and G. B. Lee, "Microfluidic cell culture chip with multiplexed medium delivery and efficient cell/scaffold loading mechanisms for high-throughput perfusion 3-dimensional cell culture-based assays," Biomed. Microdevices **13**, 415–430 (2011).
[28]A. Abbott, "Cell culture: Biology's new dimension," Nature **424**, 870–827 (2003).
[29]E. Cukierman, R. Pankov, and D. R. Stevens, "Taking cell-matrix adhesions to the third dimension," Science **294**, 1708–1712 (2001).
[30]C. G. Uhl, V. R. Muzykantov, and Y. L. Liu, "Biomimetic microfluidic platform for the quantification of transient endothelial monolayer permeability and therapeutic transport under mimicked cancerous conditions," Biomicrofluidics **12**, 014101 (2018).
[31]M. H. Wu, J. P. G. Urban, and Z. Cui, "Development of PDMS microbioreactor with well-defined and homogenous culture environment for chondrocyte 3-D culture," Biomed. Microdevices **8**, 331–340 (2006).
[32]M. H. Wu, S. B. Huang, and G. B. Lee, "Microfluidic cell culture system for drug research," Lab Chip **10**, 939–956 (2010).
[33]A. Dawson, C. Dyer, J. Macfie, J. Davies, L. Karsai, J. Greenman, and M. Jacobsen, "A microfluidic chip based model for the study of full thickness human intestinal tissue using dual flow," Biomicrofluidics **10**, 064101 (2016).
[34]L. L. Lin, Y. J. Lu, and M. L. Fang, "Computational modeling of the fluid mechanical environment of regular and irregular scaffolds," Int. J. Autom. Comput. **12**, 529–539 (2015).
[35]E. Vey and C. Roger, "Degradation mechanism of poly(lactic-co-glycolic) acid block copolymer cast films in phosphate buffer solution," Polym. Degrad. Stab. **93**, 1869–1876 (2008).
[36]A. N. Ford Versypt, D. W. Pack, and R. D. Braatz, "Mathematical modeling of drug delivery from autocatalytically degradable PLGA microspheres-A review," J. Controlled Release **165**, 29–37 (2013).
[37]L. Peng, X. L. Fang, X. L. Jia, and Y. B. Fan, "Influences of tensile load on in vitro degradation of an electrospun poly(L-lactide-co-glycolide) scaffold," Acta Biomater. **6**, 2991 (2010).
[38]X. J. Yao, J. J. Fang, and W. J. Zhang, "A further study on the analytical model for the permeability in flip-chip packaging," J. Electron. Packag. Trans. ASME. **10**, 1115 (2017).
[39]J. W. Wan, W. J. Zhang, and D. Bergstrom, "Recent advances in modeling the underfill process in flip-chip packaging," Microelectron. J. **38**, 67–75 (2006).
[40]N. K. Bawolin, M. Li, X. B. Chen, and W. J. Zhang, "Modeling material-degradation-induced elastic property of tissue engineering scaffolds," J. Biomech. Eng. **132**(11), 111001 (2010).